TimePix3 detector calibration for background radiation energy calculation and detection

Adrián Jesús Suñer Rubio, Universitat Autònoma de Barcelona (UAB), Spain

FS-DS group, CFEL, DESY

17th July-06th September 2018

Abstract

Detection is one of the most important and unnoticed topics in experimental physics. For this reason, TimePix3, a 256×256 pixel channels (55×55 μm^2) detector, which can record Time of Arrival (ToA) and Time over Threshold (ToT) simultaneously in each pixel, has been conceived as a general-purpose readout chip for Hybrid Pixel Detectors (HPDs) used in a wide range of applications, from synchrotron radiation to particle physics. Moreover, an innovative readout system called Speedy PIxel Detector Readout (SPIDR), which can deal with the high data output of 80 Mhits per chip per second needed at the field of imaging and in LHC, has been implemented to TimePix3 detector.
In this report, this prototype detctor system has been calibrated using X-ray fluorescence (XRF) in order to determine the energy of the incoming background radiation. A classification according to the topology of the spots left by the particles has made possible to distinguish different components of the background radiation: x-ray photons, alpha particles and cosmic particles.

Keywords: TimePix3, SPIDR, ToA, ToT, X-ray fluorescence (XRF), detector calibration, background radiation.

Contents

1 Introduction

Detection in experimental physics and natural sciences has generally been one of the most important, difficult and most unnoticed topics, because the goal of the experiment and its results hide it. But, how could Rutherford determine the existence of the atomic nucleus without a detector, in that case, a ZnS screen where the alpha particles that hit it created luminescent dots?
Moreover, how could DESY discover the existence of the gluon or CERN the existence of the Higgs boson without any detector? Or, how could have Barry Barish, Kip Thorne and Rainer Weiss corroborated the existence of gravitational waves predicted by Albert Einstein in his General Theory of Relativity, and, thus, win the Nobel prize of Physics in 2017, without a detection system like the one provided by LIGO?
The two main topics which DESY investigates are the application of synchrotron radiation and particle physics. But, how could we know, for example, the molecular structure of a high MW protein, the shape and composition of different nanoparticles or the existence of the elementary particles without detectors? The answer is obvious.

As we can see, in all cases the fabulous discovery hides the great importance of detectors. Even so, thanks to them science has advanced to unexpected levels.

In this context, the FS-DS (*Forschung Synchrotronstrahlung-Detektor Systeme*) group is responsible for the support and development of all detectors for photon science at DESY. Therefore, the tasks of the group include the development of novel detectors, acquisition and adaptation of the best available detectors and operation of a detector loan pool. The philosophy of the group is, whenever possible and beneficial, to collaborate with other groups at DESY, in Germany or internationally [1].

One of the detectors that the FS-DS group is working with is Timepix3, shown in Figure 1. TimePix3 is a hybrid pixel detector (HPD) readout chip, which contains 256×256 pixel channels (55×55 μm^2), with simultaneous ToA/ToT and sparse readout. It has been conceived as a general-purpose readout chip for HPDs used in a wide range of applications, from synchrotron radiation to particle physics. Furthermore, unlike other detectors, only pixels containing event information are read out [2].

Figure 1: TimePix3 detector system in which FS-DS group at DESY is working with.

One of the improvements of Timepix3 compared to its predecessor, Timepix, is that it can record time-of-arrival (ToA) and time-over-threshold (ToT) simultaneously in each pixel, while TimePix could only record ToA or ToT separately [3].

Moreover, to exploit the full capability of the TimePix3 chip, *Nikhef* has developed a compact readout system, called Speedy PIxel Detector Readout (SPIDR), that can deal with the high data output of 80 Mhits per chip per second. In order to handle the increase of the rate at which data comes in at both the experiments in the field of imaging (such as synchrotron radiation) and at the LHC, SPIDR readout system has been developed and implemented to read out TimePix3 and similar devices [4].

Nevertheless, TimePix3 with SPIDR readout system is only a prototype and the FS-DS group at DESY is tuning it up. In this context, my work has been the calibration of this detector. To carry out the calibration, the detector has been irradiated via X-ray fluorescence (XRF) using a silver x-ray anode tube as a source and different metal foils such as copper or molybdenum as XRF sources in order to know the exact energy of the photons incoming to the detector.
Then, knowing the ToT (explanation in section 2.1) distribution caused by the photons of a certain energy, we can relate ToT and Energy and, thus, calibrate the detector. Some procedures for calibrating detectors can be found in [5] and [6].
Finally, we will be able to measure the energy of the background radiation (keV scale), composed primarily of x-ray photons, cosmic particles, alpha and beta particles.

2 Theory

2.1 Detection in semiconductors

In order to detect the collision of a particle in a detector, it should be totally depleted: that is, a region within a conductive, doped semiconductor material (such as silicon, germanium, ...) where the mobile charge carriers (electrons and holes) have been forced away by an electric field.

When a low energy particle (such as a photon in the visible range of the electromagnetic spectrum) hits the detector, this creates an electron/hole pair (if it is made of silicon, the particle must have an energy greater than 1.1 eV, which is the minimum energy to create an electron/hole pair in Si), which drift in the electric field and induce an electrical signal on the metal electrodes.
High energy **photons** can interact with matter producing the *photoelectric effect*, where an inner shell electron absorb one photon and, thus is excited to the continuum, creating an electron/hole pair. An image of the process is shown in Figure 2b. Then, as explained in section 2.2, another inner shell electron can fall into the hole, generating an x-ray photon. This phenomenon is called *X-ray fluorescence (XRF)*. Nevertheless, if instead of falling, this or other more external electron is also ejected to the continuum,

the phenomenon produced is *Auger effect* and this electron is called Auger electron. These high-energy electrons will excite multiple electron/hole pairs as described below. Another way of interaction between high energy photons with matter is *Compton scattering*, which is another type of light-matter interaction, where a photon hits a valence electron gaining energy (inverse Compton scattering) or losing it (normal Compton scattering). Figure 2a represents this type of interaction.

If instead of a photon, the interacting is a **charged particle** (without high energy), it will interact electrostatically with the outer-shell electrons in a chain effect, generating electron/hole pairs while going through the material.
If this charged particle is highly energetic, it will travel through the cloud of electrons and it will be deflected by the material nuclei. During this deflection the charge is decelerated or accelerated and it therefore radiates in a continuous spectrum going from low energy photons to high energy ones. This process is called *Bremsstrahlung* and it is shown in Figure 2c.

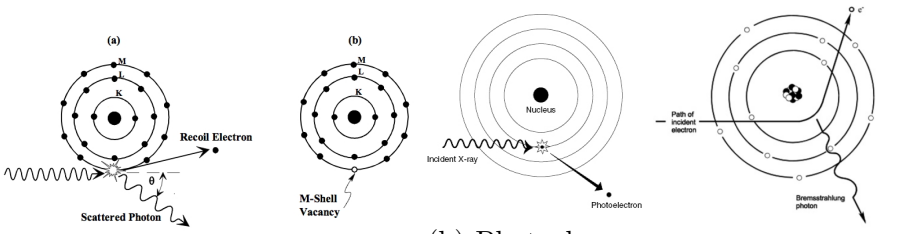

(a) Compton scattering (b) Photoelectric effect (c) Bremsstrahlung radiation

Figure 2: Three different interactions charged particles/light-matter in the x-ray energy scale. Extracted from *https://en.wikibooks.org/wiki/Basic_Physics_of_Digital_Radiography/The_Patient*.

Looking at Figure 3, Time of Arrival (**ToA**) is defined as the time when the signal, due to the hit of a particle with the detector, is differentiated with the background noise. Similarly, Time over Threshold (**ToT**) is defined as the time while the signal is above a programmable threshold.

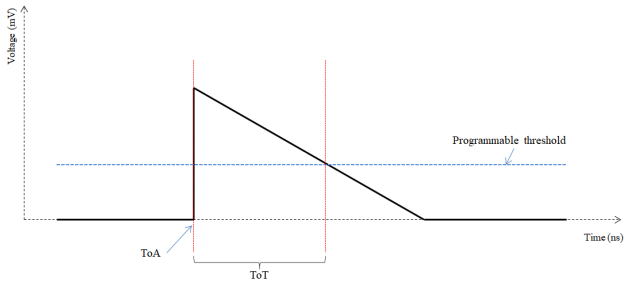

Figure 3: Ideal analog output of the detector system when a photon hits a pixel. It can be appreciated the ToA, ToT and programmable threshold variables.

It can be intuited, then, that a more energetic particle will have a higher ToT. However, in order to know the exact relationship between ToT and energy is necessary to carry out what is called *calibration*. There are many ways to calibrate a detector, but the calibration using XRF is the most viable according to availability.

2.2 X-ray fluorescence (XRF)

X-ray fluorescence (XRF) is the emission of x-ray photons when an atom is bombarded with x-ray that can displace an electron from an inner-shell orbital, normally K shell to the continuum (see Figure 4 to know the shell nomenclature) . Then, a L or M shell electron can fill it up, releasing one x-ray photon, energetically characteristic by the energy difference between both atomic orbitals. Thus, every element has its characteristic XRF energies. The photon **emitted** by the transition of a electron to an internal hole can be released in **any direction**.

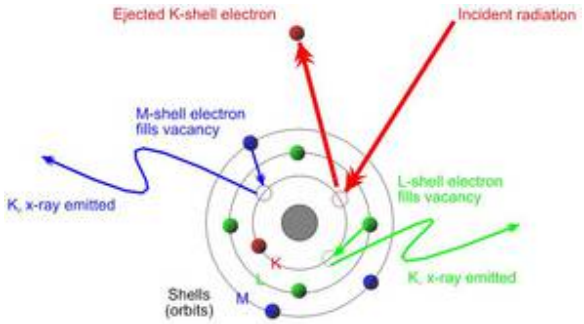

Figure 4: XRF process. Extracted from $https://www.bruker.com/products/x-ray-diffraction-and-elemental-analysis/handheld-xrf/how-xrf-works.html$.

2.3 Background radiation

Background radiation comprises all the ionizing radiation present in the environment which does not come from the deliberated introduction of radiation sources. It comes from naturally occurring radioactive decay and cosmic rays or artificially such as occupational exposure, medical exposure, nuclear fuel cycle or atmospheric nuclear testing, for example.

The **radioactive decay**, that is in the MeV scale, include the creation of α particles (He^{2+}), β particles (e^-) and γ particles (photons). The last ones can come from natural radioactive decay or due to side effect of high energy processes.

Cosmic rays are high energy particles originated in the external Universe (primary cosmic rays), which are mainly composed of nuclei such as protons, alpha particles and other heavier atomic nuclei. Only 1% of them are free electrons.

When they collide with the Earth's atmosphere, a shower of secondary particles (secondary cosmic rays) are produced. These particles almost always reach the Earth's surface in a perpendicular direction with respect it and are easily detected.

The **artificial sources** of background radiation produce always high energy photons.

Nevertheless, these particles can give all or only a part of their energy to the detector: in Table 1 we can see the energy deposited by the different components of the background radiation in the TimePix3 detector.

Table 1: Energy deposition by background radiation in TimePix3 detector. *nrd means *natural radioactive decay* and *sdHEP means *side effect of high energy processes*.

	Portion of energy given	Energy range	Energy range deposited in detector
α particles	All	MeV	MeV
β particles	All or partial	keV to few MeV	keV to few MeV
γ particles (*nrd)	Partial	MeV	>100 keV
γ particles (*sdHEP)	All	keV	<100 keV
Other cosmic particles	Partial	keV to few MeV	keV

3 Experimental procedure

3.1 Background radiation detection

In order to detect background radiation, we place the detector in order that the flat part of it stays perpendicular to the table, as shown in Figure 5. In that way, we can obtain tracks left by cosmic particles instead of few hit pixels and differentiate them from the photons, which usually left one or two hit pixels (maximum three or a square of four pixels, see section 4.1) and from the alpha particles which normally leave an almost circular bunch of hit pixels, because these particles create a lot of electron/hole pairs and deposit all their energy.

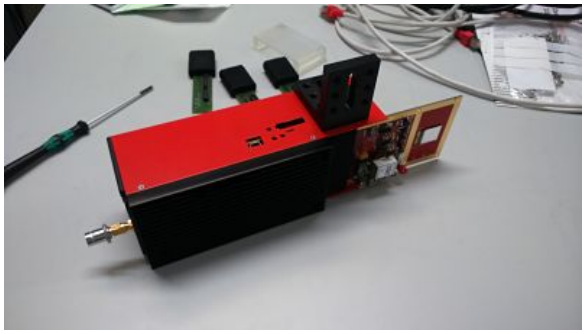

Figure 5: TimePix3 detector system positioned in order to detect background radiation.

Results and their analysis are shown in section 4.2.

3.2 Energy calibration of the detector

In order to calibrate the detector, the XRF technique was used. The scheme of the experimental setup is shown in Figure 6 and the experimental setup in Figure 7.

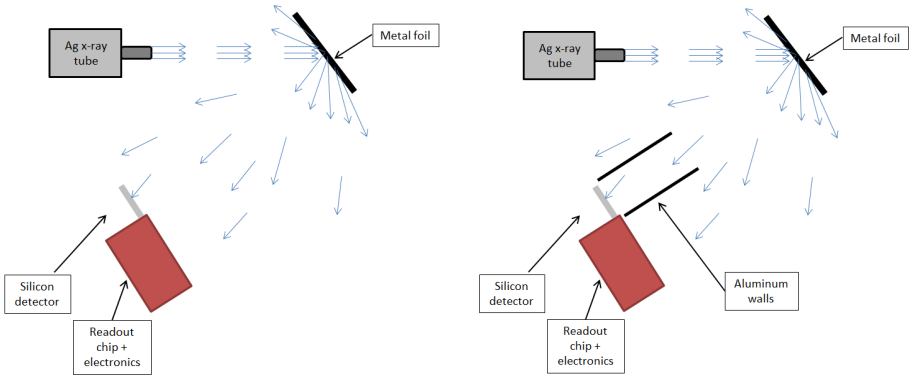

(a) First setup (b) Second setup

Figure 6: Two different setups in order to know the relation between ToT and energy. Arrows represent photon bunches.

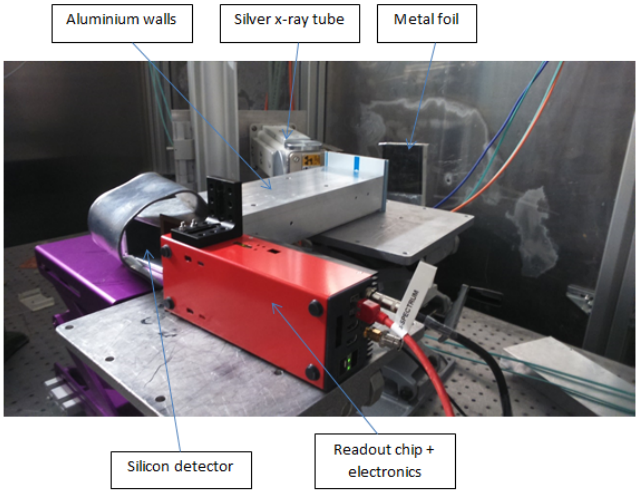

Figure 7: Second experimental setup in FS-DS *Röntgenlabor* at DESY.

As shown in Figure 6, two different configurations have been used in order to calibrate the detector. Both setups consist of a silver x-ray tube, a metal foil that can be copper or molybdenum and the TimePix3 detector with its microelectronics. However, in the second setup we put aluminum walls.

Indeed, photons leaving the x-ray tube are collimated and have a specific direction. This is because photons coming out in other directions are absorbed by the tube before leaving. Nevertheless, when these photons reach the metal foil, XRF takes place with which fluorescent photons leave in all possible directions, as it has been said in section 2.2. So, part of this radiation will directly go to the detector but most will be scattered from the walls of the laboratory and other objects of the room and, thus, with lower energy because they have deposited it in them. These photons are able to reach the detector and interfere in the good data acquisition.
That is why it is change to the second setup, which consist of introducing aluminum walls forming a hollow quadrangular prism. Thus, photons scattered from walls and other objects will be also scattered from the aluminum walls, making impossible to reach the detector. In this way, only photons that really come from the metal foil will hit the detector, showing more accurate/less noisy results.

The differences in the results between both setups are shown in section 4.3.

4 Computational work, measurements and data treatment

4.1 Classifying background radiation

We have classified the background radiation in three big groups, depending on the topology of the spot left by the particle and its energy[1]:

- **X-ray photons**: Although they don't have "size", a great approximation of the size is the cross sectional area (it depends on the photon energy, polarization and what is it interacting with), which is relatively small. In addition, the charge cloud size created is small, thus, photons only hit one pixels or two to four if they collide in the contours/corners of the pixel, as shown in Figure 8.

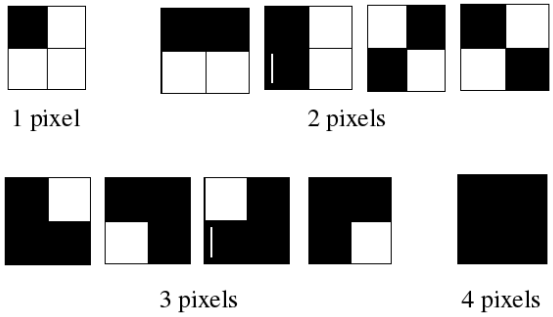

Figure 8: Different shapes done by x-ray photons in TimePix3 detector.

[1]This classification has been done with MATLAB

All these shapes can be formed because, as we have explained in section 2.1, there is a programmable trigger value. Then, for example, if a photon hits in the corner of four pixels but in one of this deposits less energy than the trigger one, this pixel is not going to be "hit". In this case, a three hit pixel shape is going to visualize.

If the program finds an event whose shape is like the ones in Figure 8, it must call this event as a "x-ray photon". Thus, we distinguish them in a topological way.

- **Cosmic particles**: In order to differentiate between x-ray photons and cosmic particles, we indicate to the program that if the shape of an event is different from the ones shown in Figure 8, it must call this event as a "cosmic particle".

- **Alpha particles**: As shown in Figures 9a and 9c, an alpha particle leaves a big spot in the detector, because it creates a lot of electron/hole pairs and deposits all its energy there.

  To differentiate them from x-ray photons, it is done the same as with the cosmic particles. Nevertheless, to distinguish between cosmic an alpha particle we can not use topology but physics: Alpha particles induce a much larger ToT value than cosmic particles. Then, establishing an arbitrary ToT threshold (3000 $\times$25 ns), if a ToT event is lower than this, it is considered as a cosmic particle, but if it is higher, it is considered an "alpha particle".

Indeed, before classifying an event between x-ray photon, cosmic particle or alpha particle, the program recognizes the shape of an event due to all the pixels involved have a **similar ToA**. The arbitrary ToA range that it is given to recognize a bunch of hit pixels as an independent event is 100 ($\times$25 ns). If two pixels have a ToA difference less than this threshold, it is considered they are a part of the same event.
It is extremely improbable that two particles arrive with a difference on ToA value less than 100 ($\times$25 ns) and the microelectronics save the ToA byte values in adjacent parts of the ToA array. Only in that strange case, the program can count one event instead of two.

4.2 Background radiation treatment

Leaving the detector as shown in Figure 5 and switching it on, it starts to take data due to the incident background radiation. After making some one minute tests in order to see the correct behaviour of the detector, we make a ten minutes test. The results of the last test are shown in Figure 9.

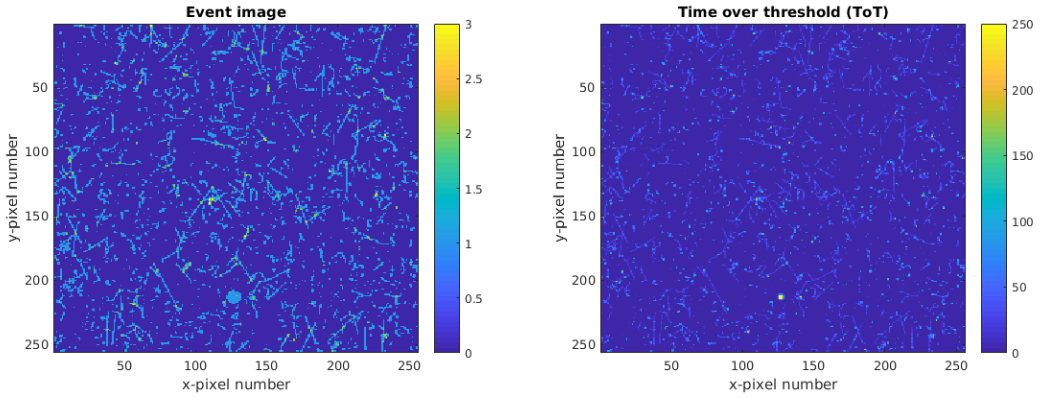

(a) Number of times a pixel has been hit (no units in colorbar)

(b) Time over Threshold at each pixel (×25 ns colorbar units)

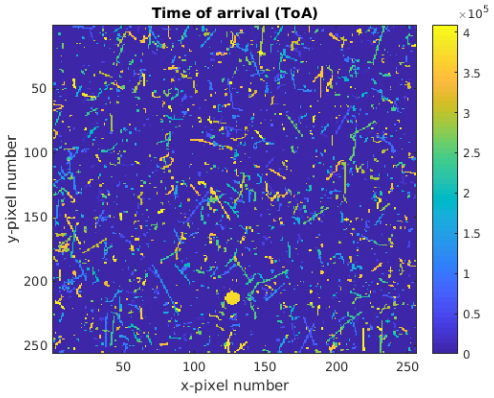

(c) Time of Arrival at each pixel (×25 ns colorbar units)

Figure 9: Different electronic parameters shown in a 10 minutes background radiation test with TimePix3 detector system.

Figure 9a shows all the events made by background radiation in a 10 minutes test. As explained in section 4.1, now we can experimentally distinguish three types of events: tracks made by cosmic particles, little marks made by photons and a big mark, which corresponds to an alpha particle.

Figure 9b shows the time over threshold values of each event. It is also known that Energy $\propto$ ToT. Thus, we can see that the big spot of Figures 9a and 9c really correspond to an alpha particle. It is also interesting that the He^{2+} particles don't give its energy isotropically, but gives more in the center of the spot because of the way the electron/hole pairs are generated (for detailed information see [7]).

We can also see in some cosmic particle tracks that the ToT values of certain pixels located at the ends are higher than the rest while in other tracks the energy is deposited isotropically. This fact is explained because cosmic particles can travel close to the speed

of light and, then, they only lose a part of its energy by coulomb repulsion while going through the silicon detector or travel at lower velocities loosing all its energy. In this case, however, the particle is slowed down while entering deeper. For this reason, at the end of the track, because it stays more time, the particle gives more energy than before.

Figure 9c shows the time of arrival (ToA) values of the events. These values are important in order to classify the events into x-ray photons, cosmic and alpha particles, as it was explained section 4.1.

Finally, using the ToA values of the events and the procedure explained in the previous section, the events of the 10 minutes background radiation test with TimePix3 detector system (Figure 9) are classified as shown in Table 2.

Table 2: Event classification of the 10 minutes background radiation test.

	X-ray photons	Cosmic particles	Alpha particles
Number of events	1365	613	1
Percentage (%)	68,974	30,975	0,051

Our goal, however, is to know the energy of these particles in order to see an compare with Table 1. In order to achieve this, we turn to section 4.3.

4.3 Data obtained with XRF

Before going into details, the theoretical XRF peaks for the two metal (molybdenum and copper) used in the setups are shown in Figure 10.

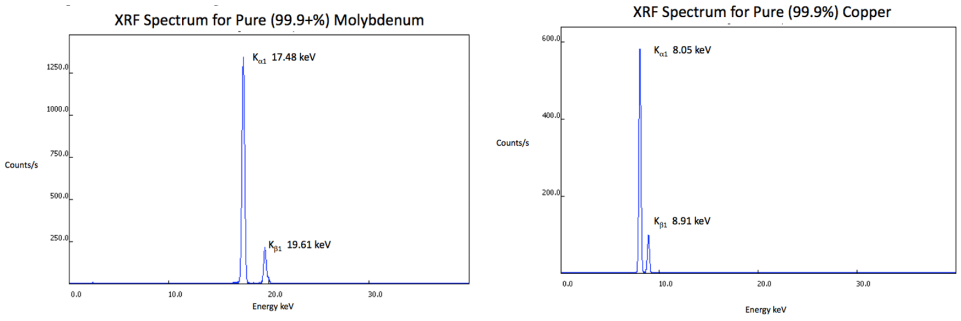

(a) Theoretical number of events vs. Energy XRF peaks of Mo

(b) Theoretical number of events vs. Energy XRF peaks of Cu

Figure 10: XRF spectra of molybdenum and copper.

As explained in subsection 3.2, the measurements have been performed with two different setups. The results are shown below.

4.3.1 First setup data

This setup corresponds to Figure 6a. Using a molybdenum sheet as metal foil, 1 second test is made in order to know the relationship between number of events vs. ToT as introduced in section 1 and studied in [5] and [6]. The distribution histogram is shown in Figure 11 (only the first 100000 hits has been selected and shown). In the same figure is also shown the number of times a pixel has been hit to compare it with Figure 9a.

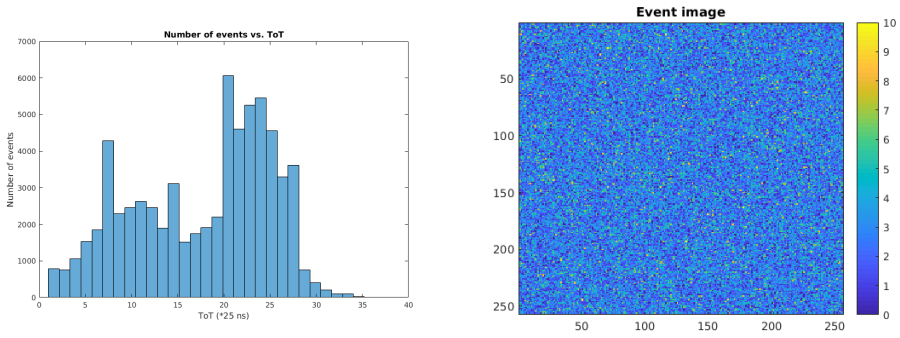

(a) Number of events vs. ToT histogram

(b) Number of times a pixel has been hit (no units in colorbar)

Figure 11: Results of a 1 second test with a Mo foil using the first setup.

Looking at Figure 11a, two peaks of Molybdenum can be distinguished. Nevertheless, there are some noisy counts that do not allow to fit properly the peaks with two Gaussian functions in order to know the their mean and standard deviation values. Indeed, in Figure 10a it is shown the two theoretical XRF peaks of Mo. With our setups, we cannot distinguish both peaks because the energy difference is lower than the resolution. In fact, we should see a shouldered peak.
In Figure 11b is shown the number of times each pixel has been hit in a **1 second** test. Compared to Figure 9a, it is clearly seen that the fluence of the x-ray photons is extraordinary higher than the background radiation. In fact, in 1 one second there are pixels hit by 10 photons (the average is between 4 and 5 hits/pixel) where in the background radiation test, in 10 minutes there were only a few pixels hit 3 times.

These are the reasons why a second setup with walls has been tested.

4.3.2 Second setup data

This setup corresponds to Figure 6b. Using aluminum walls and molybdenum and copper sheets as metal foils, two 1 second tests have been made. Distribution histograms are shown in Figure 12.

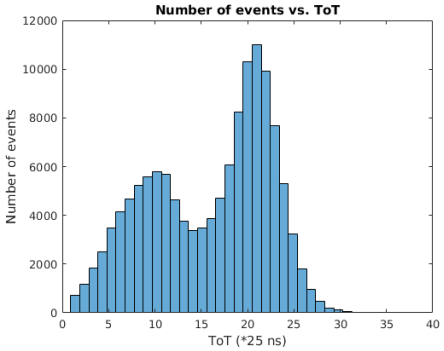

(a) Number of events vs. ToT histogram for molybdenum foil

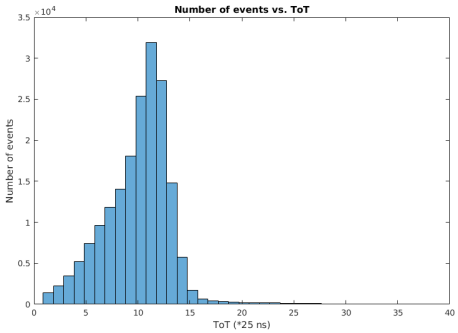

(b) Number of events vs. ToT histogram for copper foil

Figure 12: Results of 1 second tests with Mo and Cu foils using the second setup.

In Figure 12a two peaks of molybdenum are clearly shown. The noisy counts have been reduced and, thus, we are able to fit the histogram in two different ways: A Gaussian fit on the second peak ($K_{\alpha 1}$ peak) or a two-Gaussian fit, shown in Figure 13.
The fit is done in order to know its mean value, which is going to be the ToT value related with the XRF energy of the metal in order to make the Energy vs. ToT calibration.

In Figure 12b the $K_{\alpha 1}$ peak of copper is shown, while the $K_{\beta 1}$ peak is hidden inside the first due to the low resolution of the system. A Gaussian fit is going to be done and shown in Figure 14.

4.4 Energy-ToT curve

In order to make the Energy-ToT calibration curve, the gaussian fit is done and represented in Figure 13 for Mo and Figure 14 for Cu.

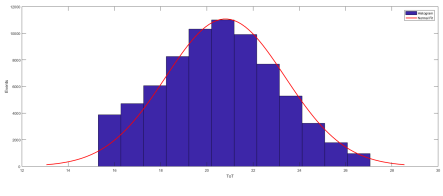

(a) Gaussian fit of the second peak in Mo XRF spectrum

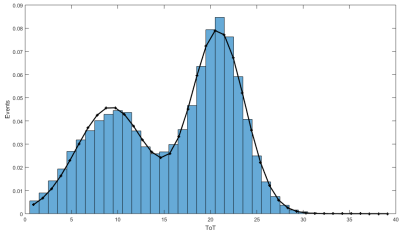

(b) Gaussian fit of both peaks in Mo XRF spectrum

Figure 13: Two different Gaussian fits of Mo XRF spectrum in order to know the ToT mean value to relate it with its XRF energy.

Although in both Figures 13a and 13b the fit is correctly done, the ToT mean values differ a bit: for Figure 13a the fitted mean value for the $K_{\alpha 1}$ peak is 20,8022 ($\times$25 ns) and for Figure 13b is 20,8287 ($\times$25 ns).
Nevertheless, a fit where all the data is taken into account is more precise than one which some counts are hidden (Figure 13a). That is why the 20,8287 ($\times$25 ns) value is chosen.

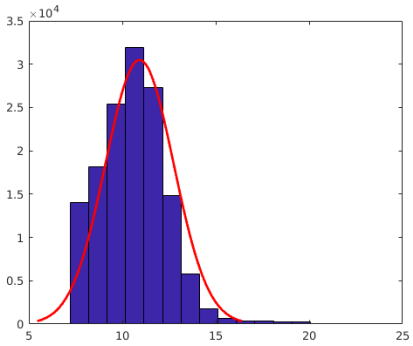

Figure 14: Gaussian fit of Cu XRF spectrum in order to know the ToT mean value to relate it with its XRF energy.

The ToT mean value obtained in the Gaussian fit for the $K_{\alpha 1}$ peak of Cu XRF spectrum is 10,9238 ($\times$25 ns).

Then, XRF energies of Figure 10 related with ToT mean values obtained experimentally are shown in Table 3.

Table 3: Energy-ToT relation of XRF spectra of Mo and Cu.

	ToT mean value (*25 ns)	$K_{\alpha 1}$ peak energy (keV)
Mo foil	20,8287	17,48
Cu foil	10,9238	8,05

IMPORTANT: Looking at [5] and [6] and comparing ToT values, we know that we are in the approximately linear Energy-ToT regimes of the calibration.

PROBLEM: Nevertheless, the TimePix3 wire bonds broke and cannot be repaired quickly. Also, there were no more sources x-ray sources and metal foils to have more data for the calibration.

For these reasons, a linear regression of data cannot be done but a straight-line going through the two experimentally obtained points, shown in Equation 1.

$$\boxed{E = 0,9520ToT - 2,3500} \tag{1}$$

4.5 Experimental calculation of the energy of background radiation

Knowing the calibration curve (Equation 1) and the ToT values of any test, we can obtain the energy of each event. Moreover, being able to distinguish the events, we are able to compare Table 1 with the experimental Table 4 took from the 10 minutes background radiation test explained in section 4.2.

Table 4: Experimental energy deposited by background radiation in TimePix3 detector in a 10 minutes test.

	Expected energy range deposited in detector	Averaged experimental energy (keV)
α particles	MeV	4711
γ particles	keV	53±46
Other cosmic particles	keV	299±260

As shown in Table 4, the expected and experimental energy values for different particles of background radiation agree with each other. Nevertheless, the standard deviation (taken here as the uncertainty) of photons and of other cosmic particle is really high. Thus, the energies are really spread out.
Figure 15 shows this energy distribution for different background radiation particles.

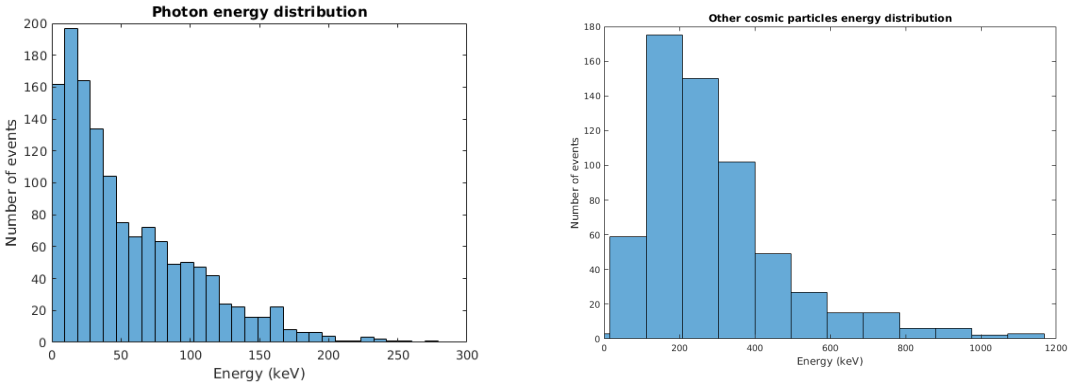

(a) Photon energy distribution

(b) Other cosmic particles energy distribution

Figure 15: Energy distribution of background radiation components.

From Figure 15 it is confirmed that all particles will have a large standard deviation value of its energy. In Figure 15a due to there is a considerable amount of events with energy greater than 70 keV and are spread out until 300 keV, the standard deviation is large, while in Figure 15b because of the big energy range, the standard deviation will also be large.

It is also seen that the amount of background radiation particles decreases with increasing energy.

5 Conclusions

Background radiation has been detected with the prototype TimePix3 detector + SPIDR readout system.
Its components have been classified in x-ray photons, alpha particles and other cosmic particles.
X-ray fluorescence (XRF) technique has been performed with molybdenum and copper foils, using an silver x-ray tube, in order to calibrate the detector.
Once the detector is calibrated, the energy of the background radiation components has been calculated and its distribution has been shown.

Table 2 shows that most of the background radiation is composed of x-ray photons. Nevertheless, there is also a big amount of other cosmic particles.
The first setup shown in Figure 6a demonstrates the existence of an amount of photons that scatter form the walls and arrive to the detector, making it necessary to put aluminum walls, as shown in Figure 6b.
Because only two metal foils have been tested, the calibration is not good, but enough to get an approximate idea of the background radiation energy.
It is clear that the amount of background radiation particles decrease with increasing energy.

Due to the wire bonds of the detector have been broken while performing XRF measurements, the next step after it is operational again is to acquire new x-ray sources and metal foils to have more data in order to do a better calibration curve. Once this has been done, a test at a DESY beamline has to be performed.

Nevertheless, the efficiency and capacity of this prototype has been demonstrated in order to create replicas on a larger scale.

Acknowledgments

I would like to thank my supervisor, David Pennicard, who has helped me patiently in this project during 8 weeks. Thanks also to Jonathan Correa, who advised me during my supervisor's holidays.
Special thanks to DESY Summer Student Programme 2018 organising team, the lecturers and DESY *Summies* for making this stay fun, enriching and unforgettable.

References

[1] DESY Photon Science. Detectors, 2018. url: `http://photon-science.desy.de/research/technical_groups/detectors/index_eng.html`.

[2] T. Poikela *et al. Timepix3, a 65K channel hybrid pixel readout chip with simultaneous ToA/ToT and sparse readout. JINST*, 9(C05013), 2014.

[3] X. Llopart R. Ballabriga M. Campbell L. Tlustos and W. Wong. *Timepix, a 65k programmable pixel readout chip for arrival time, energy and/or photon counting measurements. Nucl. Instrum. Meth.*, A 581(485), 2007.

[4] J. Visser *et al. SPIDR: a read-out system for Medipix3 & Timepix3. JINST*, 10(C12028), 2015.

[5] Jan Jakubek *et al. Pixel detectors for imaging with heavy charged particles. Nucl. Instrum. Meth.*, A 591:155–158, 2008.

[6] Jan Jakubek. *Precise energy calibration of pixel detector working in time-over-threshold mode. Nucl. Instrum. Meth.*, A 633:S262–S266, 2011.

[7] M. Campbell *et al. Study of the charge sharing in a silicon pixel detector by means of α-particles interacting with a Medipix2 device. Nucl. Instrum. Meth.*, A 591:38–41, 2008.